JOURNAL OF THERMOPHYSICS AND HEAT TRANSFER
Vol. 11, No. 3, July–September 1997

Numerical Simulation of Bhatnagar–Gross–Krook—Burnett Equations for Hypersonic Flows

Ramesh Balakrishnan* and Ramesh K. Agarwal†
Wichita State University, Wichita, Kansas 67260-0044

In this paper a kinetic-theory-based upwind algorithm for the Bhatnagar–Gross–Krook (BGK)–Burnett equations is presented. The Boltzmann equation, with the BGK approximation for the collision integral, describes the spatial and temporal variations of the second-order distribution function that forms the basis of this formulation. The second-order distribution function is derived by considering the first three terms in the Chapman–Enskog expansion and using the Navier–Stokes equations to express the material derivatives, present in the second-order terms, in terms of the spatial derivatives. The BGK–Burnett equations are derived by taking moments of the BGK–Boltzmann equation with the collision invariant vector. A kinetic wave/particle split scheme for the BGK–Burnett equations is derived by taking moments of the upwind discretized BGK–Boltzmann equation. This algorithm is applied to a hypersonic shock structure problem. This is the first time that a kinetic-theory-based method has been developed for solving the BGK–Burnett equations.

Nomenclature

C_{rms} = rms molecular velocity
c = thermal or peculiar velocity, m/s
e = total energy per unit mass, J/kg
f = velocity distribution function
$f^{(0)}$ = Maxwellian distribution function
$\boldsymbol{G}$ = flux vector
$\boldsymbol{G}^B$ = BGK–Burnett flux vector
$\boldsymbol{G}^i$ = inviscid component of the flux vector
$\boldsymbol{G}^v$ = viscous component of the flux vector
I = internal energy caused by nontranslational degrees of freedom
I_0 = average internal energy caused by nontranslational degrees of freedom
$J(f, f)$ = collision integral
j = coordinate of the grid point
k = thermal conductivity
L = characteristic length
$\mathring{m}$ = mass flux
n = time level
Pr = Prandtl number
p = pressure, N/m^2
$\boldsymbol{Q}$ = field vector
q_x = heat flux in the x direction, J/m^2
q_x^B = BGK–Burnett heat flux component
q_x^{N-S} = Navier–Stokes heat flux component
R = gas constant, N-m/kg-K
T = temperature, K
t = time, s
u = fluid velocity, m/s
x = distance along the x axis
$\boldsymbol{\beta}$ = $1/2RT$
γ = ratio of specific heats
Δ = increment in value
$\boldsymbol{\lambda}$ = mean free path
λ_∞ = freestream mean free path
μ = molecular coefficient of viscosity
ν = collision frequency
ξ = Knudsen number, defined as λ/L
ρ = density, kg/m^3
τ_{xx} = normal stress, N/m^2
τ_{xx}^B = BGK–Burnett stress component
τ_{xx}^{N-S} = Navier–Stokes stress component
$\boldsymbol{\Psi}$ = collision invariant vector

Superscripts

a = acoustic flux
B = BGK–Burnett flux
c = particle flux
v = viscous flux

I. Introduction

IN one of the earliest attempts to solve the Burnett equations, Fiscko and Chapman[1] solved the hypersonic shock structure problem by relaxing an initial solution to steady state. They obtained solutions for a variety of Mach numbers and concluded that the Burnett equations do indeed describe the normal shock structure better than the Navier–Stokes equations at high Mach numbers. They conjectured that the reasons for the failure of the Navier–Stokes equations could be any or all of the following assumptions in deriving the equations: 1) linear stress–strain relations dependent only on the velocity gradient, 2) linear heat flux dependent only on the temperature gradient, 3) zero bulk viscosity, and 4) valid for very small Knudsen numbers (continuum gas flow).

Fiscko and Chapman,[1] however, experienced stability problems when they made the grids progressively finer. This was predicted by Bobylev,[2] who showed that the linearized conventional Burnett equations are unstable to small wavelength disturbances. In a subsequent attempt, Zhong[3] showed that the equations could be stabilized by adding a few ad hoc super-Burnett terms (linear third-order terms, to maintain second-order accuracy) to the stress and heat transfer terms in the Burnett equations. This set of equations was termed the augmented Burnett equations. The augmented Burnett equations did not present any stability problems when they were used to compute the flow parameters in the hypersonic shock structure and hypersonic blunt body problems. However, attempts at computing the flowfields for blunt body wakes and flat plate

Presented as Paper 96-0602 at the AIAA 34th Aerospace Sciences Meeting, Reno, NV, Jan. 15–19, 1996; received Feb. 14, 1996; revision received March 17, 1997; accepted for publication March 19, 1997.

*Graduate Research Assistant, Department of Aerospace Engineering. Member AIAA.

†Bloomfield Distinguished Professor and Chairman, Department of Aerospace Engineering. Fellow AIAA.

boundary layers, even with the augmented Burnett equations, have not been entirely successful. It has been noted that the linear stability analysis alone is not sufficient to explain the instability of the Burnett equations with increasing Knudsen numbers as this analysis does not take into account many nonlinear terms, products of first- and higher-order derivatives, that are present in the Burnett equations.[4,5] It has also been conjectured that this instability may be because the Burnett equations violate the second law of thermodynamics at higher Knudsen numbers.

The main objectives of the present work are as follows:

1) To formulate a methodology for deriving and integrating a new set of entropy consistent Bhatnagar–Gross–Krook (BGK)–Burnett equations that can be extended to higher dimensions.

2) To check if the constitutive relations for the BGK–Burnett stress and heat transfer correctly model the flow properties at high Knudsen numbers.

3) To computationally check if the BGK-Burnett equations are stable to small wavelength disturbances.

The highly nonlinear nature of the collision integral in the Boltzmann equation presents the biggest hurdle in devising a second-order distribution function. This problem is circumvented by representing the collision integral in the BGK form. This approximation assumes that any slight departure from the equilibrium distribution will eventually settle down to the equilibrium distribution exponentially. This approximation also assumes that the gas is dilute, and the collision processes are predominantly binary in nature. Since only binary collisions are considered, the time taken for the nonequilibrium distribution to settle down to the equilibrium level is equal to the reciprocal of the collision frequency. The exact closed-form analytical expression for the distribution function[6] is derived by considering the first three terms of the Chapman–Enskog expansion. Moments of the BGK–Boltzmann equation, using the second-order distribution function, with the collision invariant vector yield the BGK–Burnett equations. In this formulation we assume that the molecules are hard elastic spheres with no intermolecular forces acting between them.

In deriving the second-order distribution function, an as yet unanswered question is the approximation for the material derivatives that appear in the second-order terms. The first- and second-order distribution functions were obtained iteratively by perturbation analysis of the one-dimensional BGK–Boltzmann equation.[6] In this analysis the Euler equations were used to approximate the material derivatives in the first-order distribution function. Moments of the first-order distribution function with the collision invariant vector yield the Navier–Stokes equations. To keep in step with the iterative refinement technique, it was conjectured that the Navier–Stokes equations be used to approximate the material derivatives in the second-order terms. It has been shown that this formulation does not violate Boltzmann's H-theorem, thereby ensuring a positive entropy gradient.[6,7] The BGK–Burnett equations contain all of the stress and heat transfer terms reported by Fiscko and Chapman[1] and these equations have additional third-order derivatives that are similar to the third-order derivatives in the super-Burnett terms.

To ensure that the entropy gradient remains positive throughout the flowfield, a set of boundary conditions has been derived using the Gibbs entropy equation. On applying this equation to the steady one-dimensional Navier–Stokes equations, it can be shown that the entropy production rate is always positive, provided the stress and heat transfer terms become vanishingly small at stations far upstream and downstream of the shock. On applying the same methodology to the steady one-dimensional BGK–Burnett equations, it was found that a positive entropy production can be ensured only by setting the heat transfer terms to zero at stations far upstream and downstream of the shock. This necessitates setting the derivatives of the velocity and temperature to zero at the ends of the control volume enclosing the shock.

Acheson and Agarwal[8] have shown that a kinetic wave/particle split (KWPS) algorithm for the Euler equations is robust and computationally efficient. This was also evidenced when the KWPS scheme was applied to the Navier–Stokes equations.[9] The kinetic-theory-based upwind schemes make use of the fact that the upwind difference equations for Euler, Navier–Stokes, and Burnett equations can be obtained by taking moments of the upwind-differenced Boltzmann equation. In this class of solvers, flux splitting is performed at the Boltzmann level. An important feature of these schemes is the ease with which they can be extended to include higher-order upwind schemes. The novel BGK–Burnett equations are solved using the KWPS scheme.[10] Numerical computations have been carried out for a hypersonic shock structure problem to assess the computational accuracy and efficiency of the KWPS upwind algorithm when applied to the BGK–Burnett equations. The results of the hypersonic shock-structure computations indicate that the present formulation ensures a positive entropy change for a wide range of grid points and Knudsen numbers (based on the length of the control volume enclosing the shock).

II. Second-Order Distribution Function

The second-order distribution function is obtained by considering the first three terms in the Chapman–Enskog expansion. The one-dimensional Boltzmann equation can be written as follows, using the BGK approximation for the collision integral $J(f, f)$:

$$\frac{\partial f}{\partial t} + v\frac{\partial f}{\partial x} = J(f, f) = \nu[f^{(0)} - f] \tag{1}$$

The variables in Eq. (1) are nondimensionalized as

$$\hat{x} = \frac{x}{L}, \qquad \hat{v} = \frac{v}{C_{\mathrm{rms}}}, \qquad \hat{t} = \frac{tC_{\mathrm{rms}}}{L}, \qquad \hat{\nu} = \frac{\nu\boldsymbol{\lambda}_\infty}{C_{\mathrm{rms}}}$$

On substituting the nondimensional variables, Eq. (1) takes the following form:

$$\xi\left(\frac{\partial f}{\partial \hat{t}} + \hat{v}\frac{\partial f}{\partial \hat{x}}\right) = \hat{\nu}[f^{(0)} - f] \tag{2}$$

The Chapman–Enskog expansion for the second-order distribution function is of the form $f = f^{(0)} + \xi f^{(1)} + \xi^2 f^{(2)}$, where $f^{(0)}$ denotes the equilibrium distribution function, $f^{(1)}$ denotes the first-order term in the distribution function, and $f^{(2)}$ denotes the second-order term. Introducing this form of the distribution function into the nondimensional, one-dimensional BGK–Boltzmann equation and equating like powers of ξ yields the following equation for $f^{(2)}$:

$$f^{(2)} = -\left(\frac{1}{\xi\nu}\right)\left\{\frac{\partial}{\partial t}[f^{(1)}] + v\frac{\partial}{\partial x}[f^{(1)}]\right\} \tag{3}$$

Expressing $f^{(2)}$ in terms of $f^{(1)}$, in a manner similar to the derivation of the first-order distribution function,[9] results in the following expressions:

$$f^{(2)} = \Phi^{(2)} f^{(1)} = \Phi^{(2)}\Phi^{(1)} f^{(0)} \tag{4a}$$

$$\Phi^{(2)} = \Phi^{(1)} - \frac{1}{\xi\nu}\left(\frac{\partial}{\partial t}[\ell n[\Phi^{(1)}]] + v\frac{\partial}{\partial x}[\ell n[\Phi^{(1)}]]\right) \tag{4b}$$

On substituting $\Phi^{(2)}$ in the Chapman–Enskog expansion for the distribution function, the following expression is obtained:

$$f = f^{(0)}[1 + \xi\Phi^{(1)} + \xi^2[\Phi^{(1)}]^2] - \frac{\xi^2 f^{(0)}}{\xi\nu}\left\{\frac{\partial}{\partial t}[\Phi^{(1)}] + v\frac{\partial}{\partial x}[\Phi^{(1)}]\right\} \tag{5}$$

In the previous expression, the last term involving the partial differential equation in $\Phi^{(1)}$ needs to be evaluated. Various methods have been devised to evaluate $f^{(2)}$ (Ref. 6). These methods make use of the physical premise that the field vector $\boldsymbol{Q}$ is the same for the Euler, Navier–Stokes, and BGK–Burnett equations. Accordingly, the moments of the distribution function with the collision invariant vector $\boldsymbol{\Psi}$ must be the same, irrespective of the form of the distribution function. Hence, moments of the additional terms in the distribution function with the collision invariant vector must be zero.

It has been shown that the moment of the first-order term with the collision invariant vector is zero.[9] Likewise, moments of the second-order term in the distribution function with the collision invariant vector must be equal to zero. Hence, we obtain the following equation:

$$\langle \Psi, f^{(0)}[[\Phi^{(1)}]^2 + \Theta]\rangle = \int_0^{\infty}\int_{-\infty}^{\infty} \Psi f^{(0)}[[\Phi^{(1)}]^2 + \Theta]\,\mathrm{d}v\,\mathrm{d}I = 0 \tag{6}$$

where

$$\Psi = \left(1\,vI + \frac{v^2}{2}\right)^T \quad\text{and}\quad \Theta = -\frac{1}{\xi\nu}\left\{\frac{\partial}{\partial t}[\Phi^{(1)}] + v\frac{\partial}{\partial x}[\Phi^{(1)}]\right\}$$

In the following method, the term Θ is evaluated by using the Navier–Stokes equations to approximate the material derivatives. The complete expression for the second-order distribution function is not given here because of space limitations. The exact expression for the second-order distribution function is given by Balakrishnan and Agarwal.[6]

III. BGK–Burnett Equations

The BGK–Burnett equations are derived by taking moments of the BGK–Boltzmann equation with the collision invariant vector. The second-order Chapman–Enskog asymptotic expansion derived in the previous section is substituted in the BGK–Boltzmann equation and the moments of each of the terms are evaluated as follows:

$$\frac{\partial}{\partial t}\langle\Psi, f^{(0)} + \xi f^{(1)} + \xi^2 f^{(2)}\rangle + \frac{\partial}{\partial x}\langle\Psi, v[f^{(0)} + \xi f^{(1)} + \xi^2 f^{(2)}]\rangle = \langle\Psi, \nu[f^{(0)} - f]\rangle \tag{7}$$

It has been shown that $\langle\Psi, \xi f^{(1)}\rangle = 0$, $\langle\Psi, \xi^2 f^{(2)}\rangle = 0$; therefore, $\langle\Psi, \nu[f^{(0)} - f]\rangle = 0$ (Ref. 9). Consequently, on evaluating the moments, the one-dimensional BGK–Burnett equations can be expressed in conservation law form as

$$\frac{\partial \boldsymbol{Q}}{\partial t} + \frac{\partial \boldsymbol{G}^i}{\partial x} + \frac{\partial \boldsymbol{G}^v}{\partial x} + \frac{\partial \boldsymbol{G}^B}{\partial x} = 0 \tag{8}$$

where

$$\boldsymbol{Q} = \begin{bmatrix}\rho\\ \rho u\\ \rho e\end{bmatrix},\quad \boldsymbol{G}^i = \begin{bmatrix}\rho u\\ p + \rho u^2\\ pu + \rho u e\end{bmatrix},\quad \boldsymbol{G}^v = \begin{bmatrix}0\\ -\tau_{xx}^{\mathrm{N-S}}\\ q_x^{\mathrm{N-S}} - u\tau_{xx}^{\mathrm{N-S}}\end{bmatrix}$$

The N–S expressions for the heat flux $q_x^{\mathrm{N-S}}$ and the normal stress $\tau_{xx}^{\mathrm{N-S}}$ are given by

$$q_x^{\mathrm{N-S}} = -k\left(\frac{\partial T}{\partial x}\right) \quad\text{and}\quad \tau_{xx}^{\mathrm{N-S}} = \mu\left(\frac{\partial u}{\partial x}\right) \tag{9}$$

From the viscous flux vector, the following relations are obtained for k and μ:

$$k = \left(\frac{\gamma}{\gamma - 1}\right)\frac{pR}{\nu} \quad\text{and}\quad \mu = \frac{p}{\nu} \tag{10}$$

The BGK–Burnett stress and heat transfer terms can be expressed as

$$\begin{aligned}\tau_{xx}^B = {} & -\theta_0\frac{\rho}{\beta^4\nu^2}\left(\frac{\partial\beta}{\partial x}\right)^2 - \theta_1\frac{\rho}{\beta\nu^2}\left(\frac{\partial u}{\partial x}\right)^2 \\ & - \theta_2\frac{\rho}{\beta^2\nu^2}\left(\frac{\partial\beta}{\partial x}\right)\frac{\mathrm{D}u}{\mathrm{D}t} - \theta_3\frac{\rho}{\beta\nu^2}\frac{\mathrm{D}}{\mathrm{D}t}\left(\frac{\partial u}{\partial x}\right) \\ & - \theta_4\frac{\rho}{\beta^2\nu^2}\left(\frac{\partial u}{\partial x}\right)\frac{\mathrm{D}\beta}{\mathrm{D}t} - \theta_5\frac{\rho}{\beta^3\nu^2}\left(\frac{\partial^2\beta}{\partial x^2}\right)\end{aligned} \tag{11}$$

$$\begin{aligned}q_x^B = {} & \theta_{12}\frac{\rho}{\beta^3\nu^2}\frac{\mathrm{D}}{\mathrm{D}t}\left(\frac{\partial\beta}{\partial x}\right) + \theta_{13}\frac{\rho}{\beta^4\nu^2}\left(\frac{\partial\beta}{\partial x}\right)\frac{\mathrm{D}\beta}{\mathrm{D}t} \\ & + \theta_{14}\frac{\rho}{\beta\nu^2}\left(\frac{\partial u}{\partial x}\right)\frac{\mathrm{D}u}{\mathrm{D}t} + \theta_{15}\frac{\rho}{\beta^2\nu^2}\left(\frac{\partial^2 u}{\partial x^2}\right) \\ & + \theta_{16}\frac{\rho}{\beta^3\nu^2}\left(\frac{\partial u}{\partial x}\right)\left(\frac{\partial\beta}{\partial x}\right)\end{aligned} \tag{12}$$

$$\begin{aligned}\tau_{xx}^B = {} & -\frac{\mu^2}{p}\left[2(\theta_1 - \theta_3)\left(\frac{\partial u}{\partial x}\right)^2 + 2\theta_3\frac{RT}{\rho^2}\left(\frac{\partial\rho}{\partial x}\right)^2\right. \\ & - 2\theta_3\frac{RT}{\rho}\left(\frac{\partial^2\rho}{\partial x^2}\right) - 4\left(\frac{\theta_3}{2} + \theta_5\right)R\left(\frac{\partial^2 T}{\partial x^2}\right) + 8\left(\frac{\theta_0}{2} + \frac{\theta_2}{4}\right. \\ & \left.\left. + \theta_5\right)\frac{R}{T}\left(\frac{\partial T}{\partial x}\right)^2 + 2(\theta_2 - \theta_3)\frac{R}{\rho}\left(\frac{\partial\rho}{\partial x}\right)\left(\frac{\partial T}{\partial x}\right)\right] \\ & - \frac{\mu^3}{p^2}\left[-2\theta_2 R\left(\frac{\partial T}{\partial x}\right)\left(\frac{\partial^2 u}{\partial x^2}\right) - 2\theta_3\frac{RT}{\rho}\left(\frac{\partial\rho}{\partial x}\right)\left(\frac{\partial^2 u}{\partial x^2}\right)\right. \\ & \left. + 2\theta_3 RT\left(\frac{\partial^3 u}{\partial x^3}\right)\right]\end{aligned} \tag{13}$$

$$\boldsymbol{G}^B = \begin{bmatrix} 0 \\ \theta_0\frac{\rho}{\beta^4\nu^2}\left(\frac{\partial\beta}{\partial x}\right)^2 + \theta_1\frac{\rho}{\beta\nu^2}\left(\frac{\partial u}{\partial x}\right)^2 + \theta_2\frac{\rho}{\beta^2\nu^2}\left(\frac{\partial\beta}{\partial x}\right)\frac{\mathrm{D}u}{\mathrm{D}t} + \theta_3\frac{\rho}{\beta\nu^2}\frac{\mathrm{D}}{\mathrm{D}t}\left(\frac{\partial u}{\partial x}\right) + \theta_4\frac{\rho}{\beta^2\nu^2}\left(\frac{\partial u}{\partial x}\right)\frac{\mathrm{D}\beta}{\mathrm{D}t} + \theta_5\frac{\rho}{\beta^3\nu^2}\left(\frac{\partial^2\beta}{\partial x^2}\right) \\ \theta_6\frac{\rho u}{\beta^4\nu^2}\left(\frac{\partial\beta}{\partial x}\right)^2 + \theta_7\frac{\rho u}{\beta\nu^2}\left(\frac{\partial u}{\partial x}\right)^2 + \theta_8\frac{\rho u}{\beta^2\nu^2}\left(\frac{\partial\beta}{\partial x}\right)\frac{\mathrm{D}u}{\mathrm{D}t} + \theta_9\frac{\rho u}{\beta\nu^2}\frac{\mathrm{D}}{\mathrm{D}t}\left(\frac{\partial u}{\partial x}\right) + \theta_{10}\frac{\rho u}{\beta^2\nu^2}\left(\frac{\partial u}{\partial x}\right)\frac{\mathrm{D}\beta}{\mathrm{D}t} + \theta_{11}\frac{\rho u}{\beta^3\nu^2}\left(\frac{\partial^2\beta}{\partial x^2}\right) \\ + \theta_{12}\frac{\rho}{\beta^3\nu^2}\frac{\mathrm{D}}{\mathrm{D}t}\left(\frac{\partial\beta}{\partial x}\right) + \theta_{13}\frac{\rho}{\beta^4\nu^2}\left(\frac{\partial\beta}{\partial x}\right)\frac{\mathrm{D}\beta}{\mathrm{D}t} + \theta_{14}\frac{\rho}{\beta\nu^2}\left(\frac{\partial u}{\partial x}\right)\frac{\mathrm{D}u}{\mathrm{D}t} + \theta_{15}\frac{\rho}{\beta^2\nu^2}\left(\frac{\partial^2 u}{\partial x^2}\right) + \theta_{16}\frac{\rho}{\beta^3\nu^2}\left(\frac{\partial u}{\partial x}\right)\left(\frac{\partial\beta}{\partial x}\right)\end{bmatrix}$$

Table 1 BGK–Burnett coefficients

	$\gamma = 1.4$	$\gamma = 1.66$
$\boldsymbol{\theta}_0$	−3.5	−2.515
$\boldsymbol{\theta}_1$	1.509	1.336
θ_2	5	167.5
θ_3	0.8	0.67
θ_4	0	0
θ_5	1	0.508
θ_6	−3.5	−2.515
θ_7	1.509	1.336
θ_8	5	167.5
θ_9	0.8	0.67
θ_{10}	0	0
θ_{11}	1	0.508
θ_{12}	−0.875	−0.629
θ_{13}	0.625	0.625
θ_{14}	−1	−0.508
θ_{15}	−0.4	−0.005
θ_{16}	−3.375	−2.149

$$
\begin{aligned}
q_x^B = \frac{\mu^2}{\rho}\Bigg\{ & 4[\boldsymbol{\theta}_{12}(\gamma-1)+\theta_{15}]\left(\frac{\partial^2 u}{\partial x^2}\right) - 4\left[\theta_{12}(\gamma-2)\right. \\
& \left. + \theta_{13}(\gamma-1) + \frac{\theta_{14}}{2} + \theta_{16}\right]\frac{1}{T}\left(\frac{\partial T}{\partial x}\right)\left(\frac{\partial u}{\partial x}\right) \\
& - 2\frac{\theta_{14}}{\rho}\left(\frac{\partial \boldsymbol{\rho}}{\partial x}\right)\left(\frac{\partial u}{\partial x}\right)\Bigg\} + \frac{\mu^3}{p\rho}\Bigg\{8\left[(\gamma-1)\theta_{12}\right. \\
& \left. + \frac{\theta_{13}}{2}\right]\frac{1}{T}\left(\frac{\partial T}{\partial x}\right)\left(\frac{\partial u}{\partial x}\right)^2 + 4(\gamma-1)\frac{\theta_{12}}{\rho}\left(\frac{\partial \rho}{\partial x}\right)\left(\frac{\partial u}{\partial x}\right)^2 \\
& - 8\left[(\gamma-1)\theta_{12} - \frac{\theta_{14}}{4}\right]\left(\frac{\partial u}{\partial x}\right)\left(\frac{\partial^2 u}{\partial x^2}\right) \\
& + 4\frac{\gamma\theta_{12}}{Pr}\frac{R}{\rho}\left(\frac{\partial \rho}{\partial x}\right)\left(\frac{\partial^2 T}{\partial x^2}\right) + \frac{8\gamma}{Pr}\left(\theta_{12} + \frac{\theta_{13}}{2}\right)\frac{R}{T}\left(\frac{\partial T}{\partial x}\right) \\
& \times\left(\frac{\partial^2 T}{\partial x^2}\right) - \frac{4\gamma\theta_{12}}{Pr}R\left(\frac{\partial^3 T}{\partial x^3}\right)\Bigg\}
\end{aligned}
\tag{14}
$$

Generalized expressions for $\theta_i(\gamma)$ are given in Ref. 6. The values of these coefficients are given in Table 1. Note that when the Euler equations are used to express the material derivatives, the resulting expression is of order μ^2. However, when the Navier–Stokes equations are used, the resulting terms are of order μ^3. These expressions have all of the terms present in the expressions for the conventional Burnett stress and heat transfer as reported by Fiscko and Chapman[1] when terms up to the order μ^2 are considered. When terms up to the order μ^3 are considered, the expressions contain third-order derivatives similar to those present in the super-Burnett terms[1] for stress and heat transfer.

IV. Linearized Stability Analysis

It has been shown by Bobylev[2] that the conventional Burnett equations are not stable to small wavelength disturbances. Hence, the conventional Burnett equations tend to blow up when the mesh sizes are made progressively finer. To investigate the stability aspects of the BGK–Burnett equations, a model problem is considered that studies the response of a uniform gas to a one-dimensional periodic perturbation wave. On linearizing the one-dimensional BGK–Burnett equations in a manner similar to the one followed by Welder et al.,[4] the following equation is obtained:

$$
\frac{\partial V'}{\partial t'} + M_1\frac{\partial V'}{\partial x'} + M_2\frac{\partial^2 V'}{\partial x'^2} + M_3\frac{\partial^3 V'}{\partial x'^3} + M_4\frac{\partial^4 V'}{\partial x'^4} = 0 \tag{15}
$$

where

$$
V' = (\rho' \quad u' \quad T')^T, \qquad M_1 = \begin{bmatrix} 0 & 1 & 0 \\ 1 & 0 & 1 \\ 0 & (\gamma-1) & 0 \end{bmatrix}
$$

$$
M_2 = \begin{bmatrix} 0 & 0 & 0 \\ 0 & -(3-\gamma) & 0 \\ 0 & 0 & \dfrac{\gamma}{Pr} \end{bmatrix}
$$

$$
M_3 = \begin{bmatrix} 0 & 0 & 0 \\ \dfrac{a^{(2)}}{R} & 0 & \dfrac{a^{(6)}}{R} \\ 0 & b^{(2)}(\gamma-1) & 0 \end{bmatrix}
$$

$$
M_4 = \begin{matrix} 0 & 0 & 0 \\ 0 & \dfrac{a^{(9)}}{R} & 0 \\ 0 & 0 & \dfrac{b^{(7)}(\gamma-1)}{RPr} \end{matrix}
$$

Let us assume the solution of the previous equation to be of the form

$$
V' = \bar{V}e^{i\omega x'}e^{\boldsymbol{\phi} t'} \tag{16}
$$

where $t' = (tp_0/\mu_0)$. The nondimensional initial conditions for Eq. (15) can be denoted in vector form as $V'|_{t=0} = \bar{V}e^{i\omega x'}$, where $x' = (x/L_0)$. The complex variable $\boldsymbol{\phi} = \alpha + i\boldsymbol{\beta}$, where α denotes the attenuation coefficient and β denotes the dispersion coefficient. For stability $\alpha < 0$ as L decreases, or in other words, the flow must attenuate as the Knudsen number increases. Substituting Eq. (16) in Eq. (15) and simplifying yields Eq. (17) when Euler equations are used to express the material derivatives:

$$
(\phi I + i\omega M_1 - \omega^2 M_2 - i\omega^3 M_3)V_0 e^{i\omega x'}e^{\phi t'} = 0 \tag{17}
$$

For a nontrivial solution Eq. (18) must be satisfied:

$$
|\phi I + i\omega M_1 - \omega^2 M_2 - i\omega^3 M_3| = 0 \tag{18}
$$

When the Navier–Stokes equations are used to express the material derivatives in terms of the spatial derivatives, Eq. (19) is obtained:

$$
(\phi I + i\omega M_1 - \omega^2 M_2 - i\omega^3 M_3 + \omega^4 M_4)V_0 e^{i\omega x'}e^{\phi t'} = 0 \tag{19}
$$

For nontrivial solutions Eq. (20) must be satisfied:

$$
|\phi I + i\omega M_1 - \omega^2 M_2 - i\omega^3 M_3 + \omega^4 M_4| = 0 \tag{20}
$$

The trajectory of the roots of the characteristic Eqs. (18) and (20) are plotted on the complex plane on which the real axis denotes the attenuation coefficient and the imaginary axis denotes the dispersion coefficient. For stability it is required that the roots lie to the left of the imaginary axis as the Knudsen number increases. Figures 1 and 2 show the trajectory of the roots of the characteristic equation as the Knudsen number increases. From the plots it is observed that unconditional stability is guaranteed only when Navier–Stokes equations are used to express the material derivatives in terms of the spatial derivatives.

To check if the approximations introduced in expressing the material derivatives destabilize the equations, the original

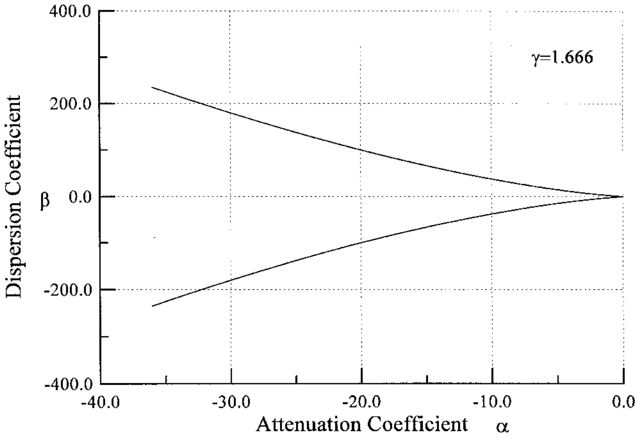

Fig. 1 Linearized stability analysis of the BGK–Burnett equations with the Euler approximation for the material derivatives in the stress and heat transfer expressions.

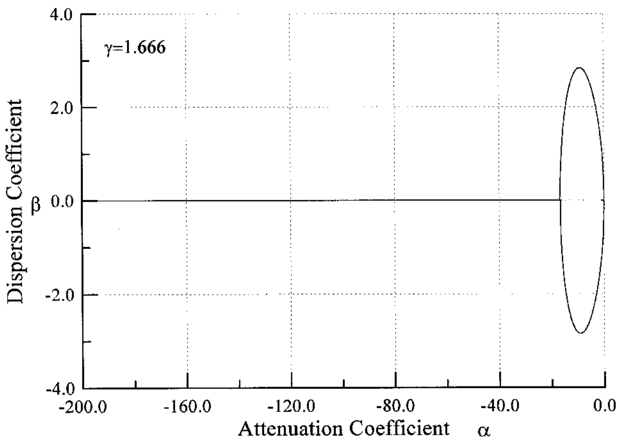

Fig. 2 Linearized stability analysis of the BGK–Burnett equations with N–S approximation for the material derivatives in the stress and heat transfer expressions.

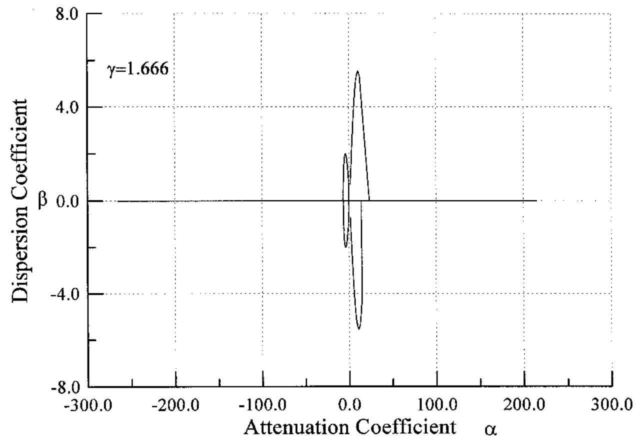

Fig. 3 Linearized stability analysis of the exact BGK–Burnett equations. Freestream Mach number equals zero.

BGK–Burnett equations are considered for stability analysis. An equation similar to Eq. (15) is obtained, where M_3 is

$$M_3 = \begin{bmatrix} 0 & 0 & 0 \\ 0 & 0 & -3\left(\boldsymbol{\theta}_1 + \theta_2 + \frac{5}{3}\theta_3\right) \\ 0 & 4(\gamma - 1)\left[\theta_4 \frac{6\gamma - 3}{8(\gamma - 1)} + \theta_5 \frac{\gamma + 3}{8(\gamma - 1)} + \theta_6 \frac{2\gamma}{8(\gamma - 1)}\right] & 0 \end{bmatrix} \tag{21}$$

The elements of M_1 and M_2 are the same as Eq. (15). The elements of M_4 are all zero. The trajectory of the roots of the characteristic equations are plotted on the complex plane as in the earlier cases. These plots are shown in Fig. 3. These plots indicate that the original BGK–Burnett equations are stable only for Knudsen numbers below 0.1. Hence, to guarantee unconditional stability, the Navier–Stokes equations must be used to express the material derivatives.

V. Kinetic Wave/Particle Flux-Splitting Algorithm

It has recently been shown by Xu et al.[11] and Perthame and Tadmor[12] that it is possible to construct less dissipative upwind schemes for Euler and Navier–Stokes equations from the BGK–Boltzmann equation. Xu et al.[11] has also proved that these schemes uphold Boltzmann's H-theorem and, hence, are total-H-diminishing (THD). Such a property eliminates the possibility of expansion shocks, especially in the upstream regions of hypersonic shock flows. To exploit the THD property of these kinetic schemes, a KWPS algorithm has been derived for the BGK–Burnett equations.

An upwind algorithm for numerically integrating the BGK–Burnett equations is derived by taking moments of the discretized BGK–Boltzmann equation with the collision invariant vector. The upwind discretization of the BGK–Boltzmann equation is shown as follows:

$$\begin{aligned} &\frac{f_j^{n+1} - f_j^n}{\Delta t} + \frac{1}{\Delta x}\left[\left(\frac{u + |u|}{2}f\right)_j - \left(\frac{u + |u|}{2}f\right)_{j-1} \right.\\ &\left. + \left(\frac{u - |u|}{2}f\right)_{j+1} - \left(\frac{u - |u|}{2}f\right)_j\right]^n + \frac{1}{\Delta x}\left[\left(\frac{c + |c|}{2}f\right)_j \right.\\ &\left. - \left(\frac{c + |c|}{2}f\right)_{j-1} + \left(\frac{c - |c|}{2}f\right)_{j+1} - \left(\frac{c - |c|}{2}f\right)_j\right]^n \\ &= [\nu[f^{(0)} - f]]_j^n \end{aligned} \tag{22}$$

Moments of Eq. (22) with $\boldsymbol{\Psi}$ yield

$$\begin{aligned} &\frac{\boldsymbol{Q}_j^{n+1} - \boldsymbol{Q}_j^n}{\Delta t} + \left(\frac{u_{j+1}\boldsymbol{Q}_{j+1} - u_{j-1}\boldsymbol{Q}_{j-1}}{2\Delta x}\right)^n \\ &- \left(\frac{|u_{j+1}|\boldsymbol{Q}_{j+1} - 2|u_j|\boldsymbol{Q}_j + |u_{j-1}|\boldsymbol{Q}_{j-1}}{2\Delta x}\right)^n \\ &+ \frac{1}{\Delta x}\left(\boldsymbol{G}_j^{ai+} - \boldsymbol{G}_{j-1}^{ai+} + \boldsymbol{G}_{j+1}^{ai-} - \boldsymbol{G}_j^{ai-}\right)^n \\ &+ \frac{1}{\Delta x}\left(\boldsymbol{G}_j^{v+} - \boldsymbol{G}_{j-1}^{v+} + \boldsymbol{G}_{j+1}^{v-} - \boldsymbol{G}_j^{v-}\right)^n \\ &+ \frac{1}{\Delta x}\left(\boldsymbol{G}_j^{B+} - \boldsymbol{G}_{j-1}^{B+} + \boldsymbol{G}_{j+1}^{B-} - \boldsymbol{G}_j^{B-}\right)^n = 0 \end{aligned} \tag{23}$$

$$
\boldsymbol{G}^{ai\pm} = \begin{bmatrix} \pm\dfrac{\rho}{2\sqrt{\pi\beta}} \\ \dfrac{p}{2} \pm \dfrac{\rho u}{2\sqrt{\pi\beta}} \\ \dfrac{pu}{2} \pm \dfrac{\rho}{2\sqrt{\pi\beta}}\left[\dfrac{p}{2}\,\dfrac{\gamma+1}{2(\gamma-1)} + \dfrac{u^2}{2}\right] \end{bmatrix} \tag{24}
$$

$$
\boldsymbol{G}^{v\pm} = \begin{bmatrix} \mp\dfrac{(3-\gamma)}{4\nu}\dfrac{\rho}{\sqrt{\beta\pi}}\dfrac{\partial u}{\partial x} \\ -\dfrac{\rho(3-\gamma)}{\nu}\left(\dfrac{1}{4\beta} \pm \dfrac{u}{4\sqrt{\beta\pi}}\right)\dfrac{\partial u}{\partial x} \mp \dfrac{\rho}{\nu}\left(\dfrac{1}{4\beta^2\sqrt{\beta\pi}}\right)\dfrac{\partial \beta}{\partial x} \\ -\dfrac{\rho(3-\gamma)}{\nu}\left[\dfrac{u}{4\beta} \pm \dfrac{u^2}{8\sqrt{\beta\pi}} \pm \dfrac{3\gamma-1}{16(\gamma-1)\beta\sqrt{\beta\pi}}\right]\dfrac{\partial u}{\partial x} + \dfrac{\rho}{\nu}\left[\dfrac{\gamma}{8\beta^3(\gamma-1)} \pm \dfrac{u}{4\beta^2\sqrt{\beta\pi}}\right]\dfrac{\partial \beta}{\partial x} \end{bmatrix} \tag{25}
$$

$$
\begin{aligned}
\boldsymbol{G}^{B\pm} = \Bigg[& [\boldsymbol{G}^{B1\pm}]\left(\frac{\partial \boldsymbol{\beta}}{\partial x}\right)^2 + [\boldsymbol{G}^{B2\pm}]\left(\frac{\partial u}{\partial x}\right)^2 \\
& + [\boldsymbol{G}^{B3\pm}]\left(\frac{\partial u}{\partial x}\right)\left(\frac{\partial \beta}{\partial x}\right) + [\boldsymbol{G}^{B4\pm}]\left(\frac{\partial \beta}{\partial x}\right)\left(\frac{\mathrm{D}u}{\mathrm{D}t}\right) \\
& + [\boldsymbol{G}^{B5\pm}]\left(\frac{\partial^2 \beta}{\partial x^2}\right) + [\boldsymbol{G}^{B6\pm}]\left(\frac{\partial^2 u}{\partial x^2}\right) \\
& + [\boldsymbol{G}^{B7\pm}]\left(\frac{\partial \beta}{\partial x}\right)\left(\frac{\mathrm{D}\beta}{\mathrm{D}t}\right) + [\boldsymbol{G}^{B8\pm}]\left(\frac{\partial u}{\partial x}\right)\left(\frac{\mathrm{D}\beta}{\mathrm{D}t}\right) \\
& + [\boldsymbol{G}^{B9\pm}]\left(\frac{\partial u}{\partial x}\right)\left(\frac{\mathrm{D}u}{\mathrm{D}t}\right) + [\boldsymbol{G}^{B10\pm}]\left[\frac{\mathrm{D}}{\mathrm{D}t}\left(\frac{\partial \beta}{\partial x}\right)\right] \\
& + [\boldsymbol{G}^{B11\pm}]\left[\frac{\mathrm{D}}{\mathrm{D}t}\left(\frac{\partial u}{\partial x}\right)\right]\Bigg]
\end{aligned} \tag{26}
$$

The 11 constituent vectors of the split BGK–Burnett flux vector are as follows:

$$
\boldsymbol{G}^{B1\pm} = \begin{bmatrix} \pm\dfrac{1}{\nu^2}\dfrac{\rho}{\beta^3\sqrt{\beta\pi}}\chi_1 \\ \dfrac{1}{\nu^2}\left(\dfrac{\rho}{\beta^4}\chi_2 \pm \dfrac{\rho u}{\beta^3\sqrt{\beta\pi}}\chi_1\right) \\ \dfrac{1}{\nu^2}\left[\pm\dfrac{\rho}{\beta^4\sqrt{\beta\pi}}\chi_3 + \dfrac{\rho u}{\beta^4}\chi_2 \pm \dfrac{\rho u^2}{\beta^3\sqrt{\beta\pi}}\left(\dfrac{\chi_1}{2}\right)\right] \end{bmatrix}
$$

$$
\boldsymbol{G}^{B2\pm} = \begin{bmatrix} \pm\dfrac{1}{\nu^2}\dfrac{\rho}{\sqrt{\beta\pi}}\chi_4 \\ \dfrac{1}{\nu^2}\left(\dfrac{\rho}{\beta}\chi_5 \pm \dfrac{\rho u}{\sqrt{\beta\pi}}\chi_4\right) \\ \dfrac{1}{\nu^2}\left[\pm\dfrac{\rho}{\beta\sqrt{\beta\pi}}\chi_6 + \dfrac{\rho u}{\beta}\chi_5 \pm \dfrac{\rho u^2}{\sqrt{\beta\pi}}\left(\dfrac{\chi_4}{2}\right)\right] \end{bmatrix}
$$

$$
\boldsymbol{G}^{B3\pm} = \begin{bmatrix} \dfrac{1}{\nu^2}\dfrac{\rho}{\beta^2}\chi_7 \\ \dfrac{1}{\nu^2}\left(\pm\dfrac{\rho}{\beta^2\sqrt{\beta\pi}}\chi_8 + \dfrac{\rho u}{\beta^2}\chi_7\right) \\ \dfrac{1}{\nu^2}\left[\dfrac{\rho}{\beta^3}\chi_9 \pm \dfrac{\rho u}{\beta^2\sqrt{\beta\pi}}\chi_8 + \dfrac{\rho u^2}{\beta^2}\left(\dfrac{\chi_7}{2}\right)\right] \end{bmatrix}
$$

$$
\boldsymbol{G}^{B4\pm} = \begin{bmatrix} \pm\dfrac{1}{\nu^2}\dfrac{\rho}{\beta\sqrt{\beta\pi}}\chi_{10} \\ \dfrac{1}{\nu^2}\left(\dfrac{\rho}{\beta^2}\chi_{11} \pm \dfrac{\rho u}{\beta\sqrt{\beta\pi}}\chi_{10}\right) \\ \dfrac{1}{\nu^2}\left[\pm\dfrac{\rho}{\beta^2\sqrt{\beta\pi}}\chi_{12} + \dfrac{\rho u}{\beta^2}\chi_{11} \pm \dfrac{\rho u^2}{\beta\sqrt{\beta\pi}}\left(\dfrac{\chi_{10}}{2}\right)\right] \end{bmatrix}
$$

$$
\boldsymbol{G}^{B5\pm} = \begin{bmatrix} \pm\dfrac{1}{\nu^2}\dfrac{\rho}{\beta^2\sqrt{\beta\pi}}\chi_{13} \\ \dfrac{1}{\nu^2}\left(\dfrac{\rho}{\beta^3}\chi_{14} \pm \dfrac{\rho u}{\beta^2\sqrt{\beta\pi}}\chi_{13}\right) \\ \dfrac{1}{\nu^2}\left[\pm\dfrac{\rho}{\beta^3\sqrt{\beta\pi}}\chi_{15} + \dfrac{\rho u}{\beta^3}\chi_{14} \pm \dfrac{\rho u^2}{\beta^2\sqrt{\beta\pi}}\left(\dfrac{\chi_{13}}{2}\right)\right] \end{bmatrix}
$$

$$
\boldsymbol{G}^{B6\pm} = \begin{bmatrix} \dfrac{1}{\nu^2}\dfrac{\rho}{\beta}\chi_{16} \\ \dfrac{1}{\nu^2}\left(\pm\dfrac{\rho}{\beta\sqrt{\beta\pi}}\chi_{17} + \dfrac{\rho u}{\beta}\chi_{16}\right) \\ \dfrac{1}{\nu^2}\left[\dfrac{\rho}{\beta^2}\chi_{18} \pm \dfrac{\rho u}{\beta\sqrt{\beta\pi}}\chi_{17} + \dfrac{\rho u^2}{\beta}\left(\dfrac{\chi_{16}}{2}\right)\right] \end{bmatrix}
$$

$$
\boldsymbol{G}^{B7\pm} = \begin{bmatrix} \dfrac{1}{\nu^2}\dfrac{\rho}{\beta^3}\chi_{19} \\ \dfrac{1}{\nu^2}\left(\pm\dfrac{\rho}{\beta^3\sqrt{\beta\pi}}\chi_{20} + \dfrac{\rho u}{\beta^3}\chi_{19}\right) \\ \dfrac{1}{\nu^2}\left[\dfrac{\rho}{\beta^4}\chi_{21} \pm \dfrac{\rho u}{\beta^3\sqrt{\beta\pi}}\chi_{20} + \dfrac{\rho u^2}{\beta^3}\left(\dfrac{\chi_{19}}{2}\right)\right] \end{bmatrix}
$$

$$
G^{B8\pm} = \begin{bmatrix} \pm \dfrac{1}{\nu^2} \dfrac{\rho}{\beta\sqrt{\beta\pi}} \chi_{22} \\ \dfrac{1}{\nu^2}\left(\dfrac{\rho}{\beta^2}\chi_{23} \pm \dfrac{\rho u}{\beta\sqrt{\beta\pi}}\chi_{22}\right) \\ \dfrac{1}{\nu^2}\left[\pm\dfrac{\rho}{\beta^2\sqrt{\beta\pi}}\chi_{24} + \dfrac{\rho u}{\beta^2}\chi_{23} \pm \dfrac{\rho u^2}{\beta\sqrt{\beta\pi}}\left(\dfrac{\chi_{22}}{2}\right)\right] \end{bmatrix}
$$

$$
G^{B9\pm} = \begin{bmatrix} \dfrac{1}{\nu^2}\rho\chi_{25} \\ \dfrac{1}{\nu^2}\left(\pm\dfrac{\rho}{\sqrt{\beta\pi}}\chi_{26} + \rho u\chi_{25}\right) \\ \dfrac{1}{\nu^2}\left[\dfrac{\rho}{\beta}\chi_{27} \pm \dfrac{\rho u}{\sqrt{\beta\pi}}\chi_{26} + \rho u^2\left(\dfrac{\chi_{25}}{2}\right)\right] \end{bmatrix}
$$

$$
G^{B10\pm} = \begin{bmatrix} 0 \\ \dfrac{1}{\nu^2}\left(\pm\dfrac{\rho}{\beta^2\sqrt{\beta\pi}}\chi_{28}\right) \\ \dfrac{1}{\nu^2}\left(\dfrac{\rho}{\beta^3}\chi_{29} \pm \dfrac{\rho u}{\beta^2\sqrt{\beta\pi}}\chi_{28}\right) \end{bmatrix}
$$

$$
G^{B11\pm} = \begin{bmatrix} \dfrac{1}{\nu^2}\left(\pm\dfrac{\rho}{\sqrt{\beta\pi}}\chi_{30}\right) \\ \dfrac{1}{\nu^2}\left(\dfrac{\rho}{\beta}\chi_{31} \pm \dfrac{\rho u}{\sqrt{\beta\pi}}\chi_{30}\right) \\ \dfrac{1}{\nu^2}\left[\pm\dfrac{\rho}{\beta\sqrt{\beta\pi}}\chi_{32} + \dfrac{\rho u}{\beta}\chi_{31} \pm \dfrac{\rho u^2}{\sqrt{\beta\pi}}\left(\dfrac{\chi_{30}}{2}\right)\right] \end{bmatrix}
$$

The coefficients χ_1–χ_{32} are functions of γ and are given in Ref. 6. The values of these variables are given in Table 2.

Table 2 Coefficients in the split BGK–Burnett flux vector

	$\gamma = 1.4$	$\gamma = 1.66$
χ_1	−1.29	−0.96
χ_2	−11.13	−10.63
χ_3	−2.92	−1.87
χ_4	0.43	0.44
χ_5	0.75	0.67
χ_6	1.64	0.69
χ_7	0	0
χ_8	−0.85	−0.59
χ_9	46.89	19.28
χ_{10}	2.5	83.75
χ_{11}	2.5	83.75
χ_{12}	40	721.39
χ_{13}	0.33	0.17
χ_{14}	0.50	0.25
χ_{15}	0.83	0.34
χ_{16}	0	0
χ_{17}	0.40	0.34
χ_{18}	−0.2	−0.002
χ_{19}	0	0
χ_{20}	0.42	0.42
χ_{21}	0.31	0.31
χ_{22}	0	0
χ_{23}	0	0
χ_{24}	0	0
χ_{25}	−0.40	−0.34
χ_{26}	−0.53	−0.45
χ_{27}	−0.50	−0.25
χ_{28}	0.25	0.25
χ_{29}	−0.44	−0.31
χ_{30}	0.40	0.34
χ_{31}	0.40	0.34
χ_{32}	0.80	0.51

VI. Entropy Considerations and Boundary Conditions

The BGK–Burnett equations are expressed in the conservation law form as

$$
\frac{\partial \boldsymbol{Q}}{\partial t} + \frac{\partial \boldsymbol{G}}{\partial x} = 0 \tag{27}
$$

The flux vector is given as

$$
\boldsymbol{G} = \begin{bmatrix} \rho u \\ \rho u^2 + p - \tau_{xx}^{\text{N-S}} - \tau_{xx}^{B} \\ \rho u e + p u + q_x^{\text{N-S}} + q_x^{B} \end{bmatrix} \tag{28}
$$

The boundary conditions for the BGK–Burnett equations are derived from the Gibbs entropy equation. The Gibbs relation can be expressed as

$$
T\nabla s = \nabla h - (1/\rho)\nabla p \tag{29}
$$

The second law of thermodynamics states that the entropy production rate must be positive for a steady-state process. Hence, the difference in entropy between a station far downstream and a station far upstream of a shock must be positive. On substituting for $(\partial h/\partial x)$ and $(\partial p/\partial x)$ from the flow equations, the following equation is obtained:

$$
\mathring{m}(s_2 - s_1) = \int_1^2 A \, \mathrm{d}x + \left.\left(-\frac{q_x}{T}\right)\right|_1^2 + \int_1^2 B \, \mathrm{d}x
$$

where

$$
A = \frac{\tau_x}{T}\left(\frac{\partial u}{\partial x}\right) \quad \text{and} \quad B = -\frac{q_x}{T^2}\left(\frac{\partial T}{\partial x}\right) \tag{30}
$$

The subscripts 1 and 2 are used to identify the upstream and downstream locations, respectively. The previous equation implies that setting the heat transfer q_x equal to zero at the ends of the control volume ensures a positive entropy gradient if A and B are positive. For the Navier–Stokes equations, a positive entropy gradient is ensured by setting the heat transfer $q_x^{\text{N-S}}$ terms equal to zero at stations 1 and 2. This is achieved by setting the derivative $(\partial T/\partial x)$ equal to zero. For the Navier–Stokes equations the integrands A and B take the form shown next. It can be seen that both A and B are positive:

$$
A = \frac{\mu}{T}\left(\frac{\partial u}{\partial x}\right)^2 \quad \text{and} \quad B = \frac{k}{T^2}\left(\frac{\partial T}{\partial x}\right)^2
$$

Although a similar analytical analysis is difficult for the Burnett equations, it has been verified computationally[9] that the integrands A and B are positive. This is ensured by setting all of the derivatives in q_x^B equal to zero at stations 1 and 2 at the ends of the control volume enclosing the shock.

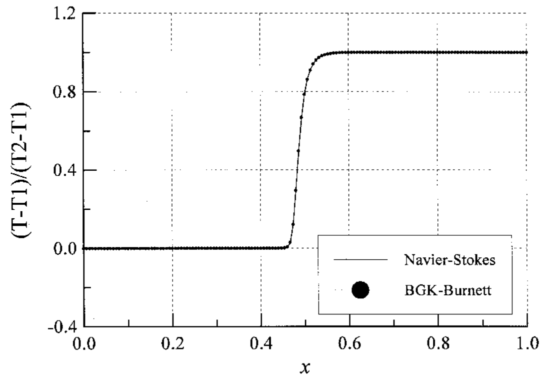

Fig. 4 Normalized temperature variation across a Mach 35 (argon) normal shock for $Kn = 0.001$. KWPS scheme with N–S equations for D( )/D*t*.

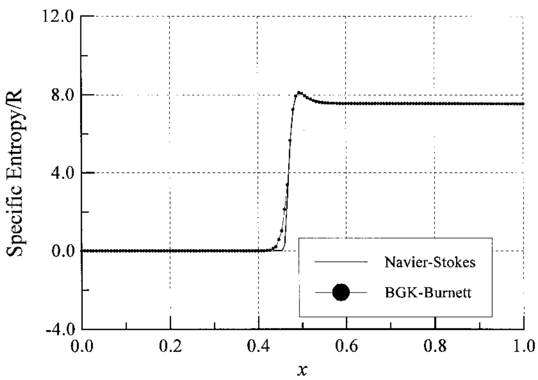

Fig. 5 Specific entropy variation across a Mach 35 (argon) normal shock for $Kn = 0.001$. KWPS scheme with N–S equations for D( )/D*t*.

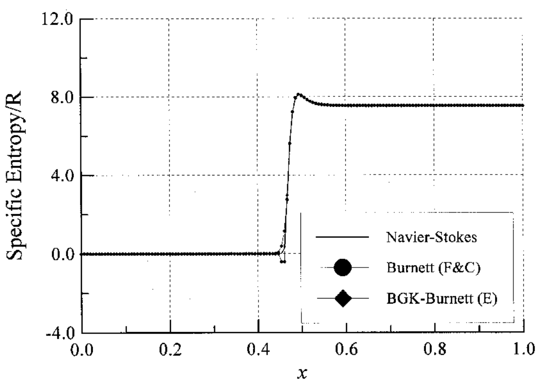

Fig. 6 Specific entropy variation across a Mach 35 (argon) normal shock for $Kn = 0.001$. Euler equations (E) are used to express D( )/D*t*.

VII. Numerical Experiments

The KWPS algorithm derived previously was applied to the hypersonic shock structure problem. The objective of this numerical experiment was to test the computational stability of the entropy-consistent BGK–Burnett equations by integrating them numerically on progressively finer grids. The scheme was applied initially to a coarse mesh of 101 grid points. The number of grid points was increased to 501. The reference parameters used are similar to those used by Zhong[3]: $T_\infty = 300$ K, $P_\infty = 1.01325 \times 10^5$ nm^{-2}, $\gamma_{\text{argon}} = 1.66$, and $\mu_{\text{argon}} = 22.7 \times 10^{-6}$ nm^{-2}.

The upstream flow conditions were specified and the downstream conditions were determined by the Rankine–Hugoniot relations. The Navier–Stokes solution was taken as the initial distribution for the BGK–Burnett equations. This smooth spatial distribution of variables was imposed on a mesh that encloses the normal shock. For this reason a control volume of length $1000\lambda_\infty$ was chosen as the reference length. This reference length is used to define the Knudsen number for the one-dimensional shock structure problem. The mean free path based on the freestream parameters is obtained from the following relation:

$$\lambda_\infty = \frac{16\mu}{5\rho_\infty\sqrt{2\pi R T_\infty}} \tag{31}$$

The solution was marched until the deviations were smaller than a preset convergence criterion. Figures 4 and 5 show comparisons of the normalized temperature and specific entropy distributions when Navier–Stokes and BGK–Burnett equations were used to compute the shock structure. The BGK–Burnett equations did not exhibit any kind of instability for a wide range of grid points. To compare the BGK–Burnett equations and the conventional Burnett equations, the hypersonic shock structure was computed by using a first-order upwind scheme for the inviscid part and central differencing the viscous and Burnett/BGK–Burnett terms. The results of these computations are shown in Fig. 6. A pronounced negative entropy spike is observed in the region upstream of the normal shock when the conventional Burnett equations are used. This negative spike occurs just before the conventional Burnett equations exhibit computational instabilities.

VIII. Conclusions

An entropy consistent set of BGK–Burnett equations has been derived from first principals. These equations have been numerically integrated using the KWPS scheme. The equations are computationally stable for the range of grid points and Knudsen numbers for which results are presented. The differences between the BGK–Burnett and Navier–Stokes results become significant at higher Knudsen numbers. This is shown by the results of the hypersonic shock structure computations.

Acknowledgments

This work has been supported by Air Force Office of Scientific Research Contract F49620-95-1-0125. The authors wish to acknowledge Len Sakell for his support and encouragement on this project.

References

[1]Fiscko, K. A., and Chapman, D. R., *Comparison of Burnett, Super-Burnett and Monte Carlo Solutions for Hypersonic Shock Structure*, Vol. 118, Progress in Aeronautics and Astronautics, AIAA, Washington, DC, 1989, pp. 374–395.

[2]Bobylev, A. V., "The Chapman-Enskog and Grad Methods for Solving the Boltzmann Equation," *Soviet Physics—Doklady*, Vol. Vol. 27, No. 1, 1982, p. 29.

[3]Zhong, X., "Development and Computation of Continuum Higher Order Constitutive Relations for High-Altitude Hypersonic Flow," Ph.D. Dissertation, Stanford Univ., Stanford, CA, 1991.

[4]Welder, W. T., Chapman, D. R., and MacCormack, R. W., "Evaluation of Various Forms of the Burnett Equations," AIAA Paper 93-3094, July 1993.

[5]Comeaux, K. A., Chapman, D. R., and MacCormack, R. W., "An Analysis of the Burnett Equations Based on the Second Law of Thermodynamics," AIAA Paper 95-0415, Jan. 1995.

[6]Balakrishnan, R., and Agarwal, R. K., "Formulation of a Second Order Distribution Function by Perturbation Analysis of the Boltzmann Equation," Dept. of Aerospace Engineering, Wichita State Univ., Wichita, KS, 1995.

[7]Agarwal, R. K., and Balakrishnan, R., "Numerical Simulation of BGK-Burnett Equations," Air Force Office of Scientific Research, Aug. 1996.

[8]Acheson, K. E., and Agarwal, R. K., ''A Kinetic Theory Based Wave/Particle Flux Splitting Scheme for Euler Equations,'' AIAA Paper 95-2178, June 1995.

[9]Balakrishnan, R., and Agarwal, R. K., ''Development of the First Order Distribution Function and a Kinetic Wave/Particle Flux Splitting Scheme for the Navier-Stokes Equations,'' Dept. of Aerospace Engineering, Wichita State Univ., Wichita, KS, 1995.

[10]Balakrishnan, R., and Agarwal, R. K., ''Development of a Kinetic Wave/Particle Flux Splitting Scheme for the Burnett Equations,'' Dept. of Aerospace Engineering, Wichita State Univ., Wichita, KS, 1995.

[11]Xu, K., Martinelli, L., and Jameson, A., ''Gas Kinetic Finite Volume Methods, Flux-Vector Splitting, and Artificial Diffusion,'' *Journal of Computational Physics*, Vol. 120, 1995, pp. 48–65.

[12]Perthame, B., and Tadmor, E., *Communications in Mathematical Physics*, Vol. 36, 1991, p. 501.